



HAL
open science

Heat Diffusion in an Optical Logic Gate Array on Silicon-on-Sapphire

H. Gualous, A. Koster, D. Pascal, S. Laval

► **To cite this version:**

H. Gualous, A. Koster, D. Pascal, S. Laval. Heat Diffusion in an Optical Logic Gate Array on Silicon-on-Sapphire. *Journal de Physique III*, 1997, 7 (3), pp.739-748. 10.1051/jp3:1997152 . jpa-00249609

HAL Id: jpa-00249609

<https://hal.science/jpa-00249609>

Submitted on 4 Feb 2008

HAL is a multi-disciplinary open access archive for the deposit and dissemination of scientific research documents, whether they are published or not. The documents may come from teaching and research institutions in France or abroad, or from public or private research centers.

L'archive ouverte pluridisciplinaire **HAL**, est destinée au dépôt et à la diffusion de documents scientifiques de niveau recherche, publiés ou non, émanant des établissements d'enseignement et de recherche français ou étrangers, des laboratoires publics ou privés.

Heat Diffusion in an Optical Logic Gate Array on Silicon-on-Sapphire

H. Gualous, A. Koster, D. Pascal and S. Laval (*)

Institut d'Électronique Fondamentale (**), Bâtiment 220, Université Paris Sud,
91405 Orsay Cedex, France

(Received 10 October 1996, accepted 13 December 1996)

PACS.42.79 Ta – Optical computers, logic elements, interconnects, switches, neural networks
PACS.42.82 Et – Waveguides, couplers and arrays
PACS 44.10 +i – Heat conduction (models, phenomenological description)

Abstract. — Designing optical logic gate array needs to reduce thermal interactions between pixels. Heat diffusion between an active pixel and its neighbours is calculated using an original method derived from the electrostatic image method. Temperature variations are calculated as a function of the distance from the pixel center. The mean temperature rises of the various pixels are estimated and thermal influence between adjacent pixels is determined.

Résumé. — Lors de la conception d'un réseau de portes logiques optiques, il faut tenir compte des interactions thermiques entre pixels. La diffusion de la chaleur entre un pixel actif et ses voisins est calculée par une méthode originale dérivée de la méthode des images en électrostatique. Les variations de température en fonction de la distance par rapport au centre du pixel sont calculées. L'élévation moyenne de température des différents pixels est estimée et l'influence thermique entre des pixels adjacents est ainsi déterminée.

Introduction

Although thermal effects are generally considered as parasitics in electronic or optoelectronic device operation, they have been widely used to demonstrate optical switching and to realize optical logic gate arrays for all-optical signal processing systems [1–8]. Heating induces changes in the optical properties of active materials through refractive index variations, and this leads to nonlinear behavior [9, 10].

However, if several devices are set on a substrate to realize an array, heat diffusion has to be reduced from one device to the other to avoid unwanted coupling between neighbour pixels.

Heat diffusion has been studied in an optical logic gate array in order to determine the importance of coupling between two adjacent pixels and to design the array in such a way that mutual influence between two pixels can be kept negligible. An original method derived from the image method in electrostatic [11] has been used and is described in this paper. It is applied to the design of a logic gate array on a silicon-on-sapphire substrate.

(*) Author for correspondence (e-mail: suzanne.laval@ief-paris-sud.fr)
(**) CNRS URA 22

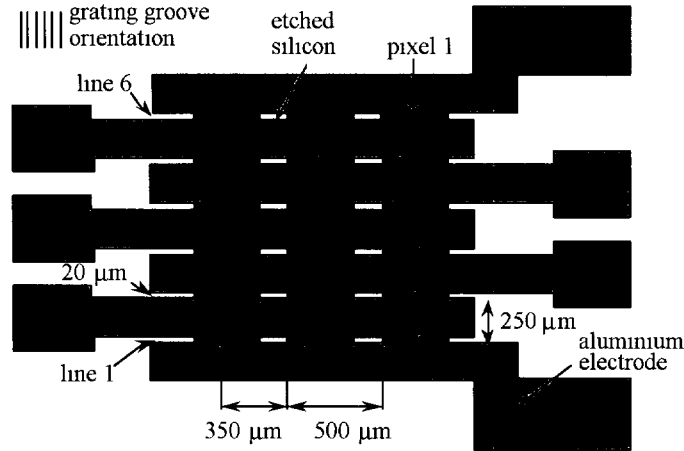


Fig. 1. — Geometry of the logic gate array

1. Nonlinear Device Array

Optical logic gate array operation has been demonstrated on silicon-on-sapphire substrate [8]. The thicknesses of the sapphire substrate and of the epitaxial silicon film are respectively $e_{\text{sub}} = 330 \mu\text{m}$ and $e_{\text{si}} = 0.6 \mu\text{m}$. Each pixel is delimited by etching the silicon film and has a length of $350 \mu\text{m}$ and a width equal to $20 \mu\text{m}$. Aluminium electrodes are deposited on each side of the pixels. The elementary array consists in 3×6 optical gates (Fig. 1).

The silicon film is used as an optical waveguide to enhance the electromagnetic field confinement and then to increase nonlinearities. Light is coupled in the waveguide through a diffraction grating fabricated by holographic insolation of a photoresist and ion milling. The period $\Lambda = 0.33 \mu\text{m}$ is chosen in such a way that only the diffracted beams in the ± 1 order can propagate in the optical waveguide. A guided mode is excited if the incident beam fulfil the resonance condition:

$$\frac{2\pi}{\lambda} \sin \theta_m \pm \frac{2\pi}{\Lambda} = \beta_m \quad (1)$$

where β_m is the propagation constant of the excited mode, θ_m the incidence angle and λ the light wavelength. Under linear regime conditions (low incident power), the resonance is observed as a dip in the curve giving the transmission light intensity as a function of the incidence angle.

When such device is illuminated with a wavelength $\lambda = 1.06 \mu\text{m}$ from a Nd:Yag laser, light is absorbed and electron-hole pairs are created. This induces in silicon a refractive index change which is proportional to the excess carrier density and then to the absorbed optical power.

$$\delta n_e = K_e \delta N \quad \text{with} \quad K_e = -9 \times 10^{-22} \text{ cm}^3 \quad (2)$$

As silicon has an indirect band gap structure, electron-hole pair recombination is accompanied by phonon emission and the temperature increase also induces variations of the refractive index:

$$\delta n_T = K_T \delta T \quad \text{with} \quad K_T = +2.4 \times 10^{-4} \text{ K}^{-1}. \quad (3)$$

The net refractive index variation is:

$$\delta n_{\text{Si}} = K_e \delta N + K_T \delta T. \quad (4)$$

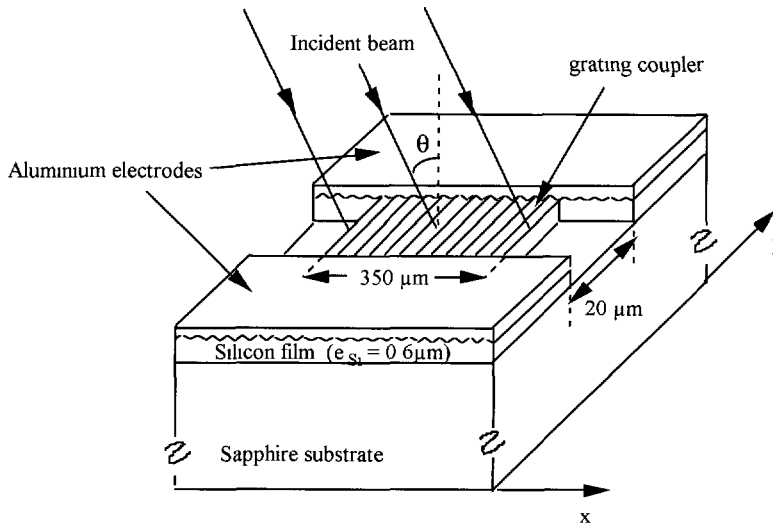


Fig. 2. — Schematic representation of a pixel.

Under c.w. illumination, or illumination with pulses much longer than the carrier lifetime, thermal effects are predominant. They can be further enhanced by Joule effect induced by photocurrent if electrodes are deposited on each side of the waveguide.

The index variations lead to nonlinear behaviour and this is used to get optical switching. If the incidence angle of the light beam is shifted with respect to resonance at low incident power, the initial device transmission is high. As the optical intensity increases, absorption leads to higher temperature and the refractive index variation compensates the initial shift from resonance. Then the transmission switches to a low level.

When such elementary devices are set into an array, heat transfer between neighbour pixels has to be minimized in order to avoid parasitic couplings. So it is important to estimate heat diffusion from one pixel to the neighbour ones.

2. Heat Diffusion from One Pixel

Let us consider a pixel represented in Figure 2. When an incident beam impinges on it, the illuminated region is heated by both optical absorption and Joule effect from the photocurrent, and heat diffuses into the structure. Heat diffusion equation has to be solved in the various materials constituting the system under consideration, taking into account continuity relations for the heat flow normal to the interfaces. Thermal conductivity is homogeneous in each media. Under stationary operation conditions with respect to time, heat diffusion equation can be written in the silicon layer as:

$$\nabla^2 T = \frac{P_Q(x, y, z)}{K_{S_1}} \tag{5}$$

where $P_Q(x, y, z)$ is the heating power sources by unit volume and K_{S_1} the thermal conductivity of silicon.

In the other media (sapphire, air, aluminium) no heat sources are present and $\nabla^2 T = 0$.

Table I. — *Thicknesses and thermal conductivities of the various materials of the structure*

Material	Thickness (μm)	Thermal conductivity ($\text{Wm}^{-1} \text{K}^{-1}$)
Silicon	0.6	160
Aluminium	0.5	200
Sapphire	330	33
Air	∞	2.4×10^{-2}

Partial derivative equations for heat diffusion are generally solved numerically using the finite difference method. This needs to define a mesh over the whole 3-dimensional structure and is time consuming. It may be convenient to develop an approximate analytical method which allows to reduce numerical calculations.

The method derived from the image method for electrostatic potential calculation [11] which consists in calculating a double or triple integral, cannot be applied directly to the problem under consideration as the silicon and aluminium layers are not continuous. However, it can lead to a good approximation if heat diffusion takes place mainly in the sapphire substrate and can be neglected in the silicon and aluminium layers.

In order to study this point, a simplified structure has been considered, consisting of a heated strip of infinite length and width equal to the interelectrode distance ($20 \mu\text{m}$). The finite difference method has been used and a variable cell mesh has been defined over the structure. The temperature is fixed to T_0 on the back face of the sapphire substrate and the temperature variations $\Delta T = T - T_0$ are calculated. As the system is symmetrical, the axis origin is fixed on the middle of the heated strip and calculation is only performed for the half structure. The thicknesses and thermal conductivities of the various materials are given in Table I. The values of the thermal conductivities are those of bulk materials.

The temperature variations are calculated at the interface between silicon and sapphire along the y direction perpendicular to the strip axis. Results are plotted in Figure 3 for $P_Q = 10 \text{ kW cm}^{-3}$. Two cases are compared: either the calculation takes into account the continuous silicon film and the aluminium electrodes (Fig. 3a), or the aluminium and the silicon underneath are replaced by air (Fig. 3b). Beyond $40 \mu\text{m}$ from the middle of the heated strip, temperature variations along the y -axis are identical in the two cases: heat diffusion in the silicon and aluminium layers is negligible. Near the heated region ($y < 40 \mu\text{m}$), the calculated difference between the realistic structure and the approximate one is about 6.6%. This value is probably overestimated as thermal conductivities of thin films may be lower than bulk material values. Furthermore, the finite length of the pixel in the experiment induces heat diffusion along the strip axis which also reduces this difference.

This calculation also showed that the temperature difference between the silicon film surface and the sapphire/silicon interface is less than 0.3%. Heat diffusion across the thin silicon layer can then be neglected.

So, within an accuracy of about 7%, the structure can be approximated by a very simple one which consists of a sapphire substrate with heat sources distributed on its surface according to pixel locations. The image method can then be applied.

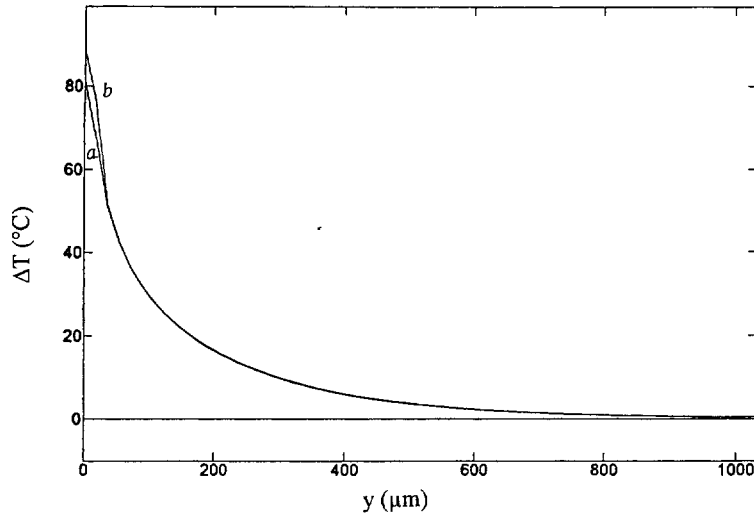


Fig. 3. — Comparison of the temperature evolution calculated along the y -axis using finite difference method: (a) with a continuous silicon film and aluminium electrodes, (b) without aluminium electrodes and silicon in the non-heated regions.

3. Thermal Influence Between Pixels

An elementary area dS is considered in a heated region of the sapphire surface, around a point $M(x, y)$ belonging to a pixel. The thermal influence from this elementary area to any other point $N(x', y')$ on the sapphire surface induces a temperature change which can be written as:

$$d[T(N) - T_0] = d\Delta T(N) = C(M, N)P_S(M)dS \quad (6)$$

where $\Delta T(N)$ is the temperature rise at point $N(x', y')$ with respect to the thermostat temperature T_0 and $P_S(M)$ is the elementary heating power density at point $M(x, y)$. The factor $C(M, N)$ characterizes the interaction between the two points and depends on their mutual distance, on the thermal conductivity and on the position of the thermostat.

The temperature increase at $N(x', y')$ is obtained by integrating over the whole heated area S :

$$\Delta T(N) = \int \int_S C(M, N)P_S(M)dS. \quad (7)$$

The problem consists in calculating the interaction coefficient $C(M, N)$. It is helpful to consider that the integral is similar to the calculation of an electrostatic potential created by a charge distribution. Correspondence between electrostatic and thermal quantities is given in Table II.

Referring to Table II, the temperature increase at $N(x', y')$ induced by the elementary surface dS around $M(x, y)$ can be written as:

$$dT = \frac{P_S dS}{4\pi r K_{sa}}, \quad (8)$$

where r is the distance between M and N and K_{sa} the sapphire thermal conductivity. As the thermal conductivity of air is 5×10^{-3} times smaller than the sapphire one, heat diffusion in air is neglected.

Table II. — *Correspondence between electrostatic and thermal quantities.*

Electrostatic quantities	Thermal quantities
potential V	temperature T
permittivity ϵ	thermal conductivity K
surface-charge density σ	surface heating density P_S
electrical charge density ρ	heating power density P_Q

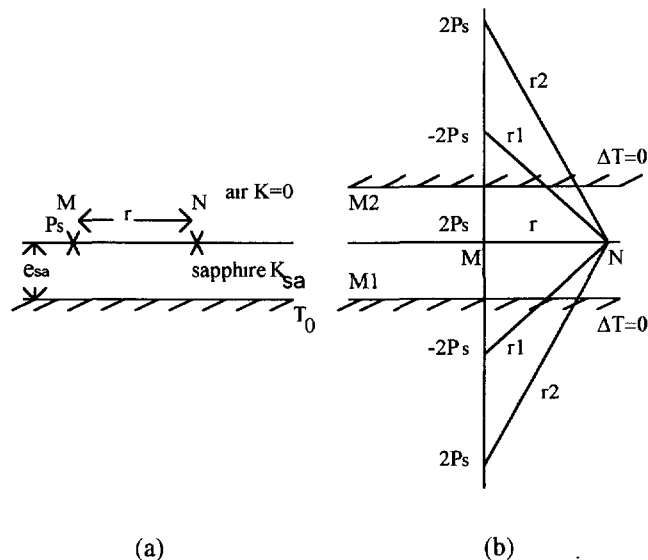


Fig. 4. — Heat sources distribution used in the image method

The temperature of the back face of the sapphire substrate is fixed by the thermostat and equal to T_0 ($\Delta T = 0$). The problem is similar to the calculation of the potential difference induced by an electrical charge set at point M in a half-plane in which a line has been set to a fixed potential. The isothermal line corresponding to the rear face of the sapphire substrate is considered as a mirror M_1 and the system is imaged with respect to the front face of the sapphire. The image of the mirror M_1 is a mirror M_2 which must also fulfil the condition $\Delta T = 0$. The heating power density has then to be equal to $2P_S$. Using the image method, virtual images of M are defined by reflection on mirrors M_1 and M_2 with heating densities alternatively positive and negative (Fig. 4). The temperature variation at $N(x', y')$ is obtained by addition of the contributions of every images:

$$d\Delta T(N) = \frac{P_S}{2\pi K_{sa}} \left[\frac{1}{r} - \frac{1}{r_1} + \frac{2}{r_2} - \dots \right] dS. \quad (9)$$

As N and M are on the substrate surface, the distance between N and the i^{th} image is $r_i^2 = r^2 + (i2e_{\text{sa}})^2$, e_{sa} being the sapphire substrate thickness. Equation (9) is then written:

$$d\Delta T(N) = \frac{P_S}{2\pi K_{\text{sa}}} \left[\frac{1}{r} + 2 \sum_{i=1}^{\infty} \frac{(-1)^i}{\sqrt{r^2 + (i2e_{\text{sa}})^2}} \right] dS. \quad (10)$$

The interaction coefficient $C(M, N)$ is equal to:

$$C(M, N) = \frac{1}{2\pi K_{\text{sa}} r} \left[1 + 2 \sum_{i=1}^{\infty} \frac{(-1)^i}{\sqrt{1 + 4i^2(e_{\text{sa}}/r)^2}} \right]. \quad (11)$$

The function $f(r/e_{\text{sa}}) = 1 + 2 \sum_{i=1}^{\infty} \frac{(-1)^i}{\sqrt{1 + 4i^2(e_{\text{sa}}/r)^2}}$ characterizes the thermostat influence.

The temperature change at any point $N(x', y')$ is given by the integral over the heated area S :

$$\Delta T(N) = \frac{1}{2\pi K_{\text{sa}}} \int \int_S \frac{1}{r} f\left(\frac{r}{e_{\text{sa}}}\right) P_S dS.$$

It is worth noting that for numerical calculations the function here above can be approximated by the analytical function $g(\frac{r}{e_{\text{sa}}}) = \exp(-a(\frac{r}{e_{\text{sa}}})^b)$ with $a = 0.924869$ and $b = 1.183895$ [13]

4. Results and Discussion

When a pixel is illuminated by the incident beam to excite a guided mode, even if the incident light intensity is uniform over the pixel, the guided intensity is non-uniform along the propagation direction. The guided light intensity exhibits a transient growth with a characteristic length of the order of $30 \mu\text{m}$ for the waveguide under consideration [12]. The absorbed power increases in this region up to its maximum value which is obtained when the guided mode reaches its stationary amplitude. In order to take into account these spatial transients, the surface heating power density, for a resonant excitation of the mode with a low incident power, is assumed to vary along the propagation direction x according to $P_S = P_{S0}(1 - e^{-x/D})$ where D is the characteristic growth length ($D = 30 \mu\text{m}$). The maximum surface heating power density P_{S0} has been estimated from experimental measurements at the switching threshold [13], for an initial angular detuning of 0.30° from resonance, taking into account the optical absorbed power and the power dissipated from Joule effect. P_{S0} is equal to 3.2 kW cm^{-2} .

The temperature distribution calculated at the silicon-sapphire interface is plotted in Figure 5. The mean temperature rise of the pixel is 24.4°C and the maximum temperature change, around the pixel center, is 26.5°C . The temperature variations in the symmetry planes of the pixel are given more accurately in Figure 6. In the transverse direction, parallel to the y -axis, the temperature changes are symmetrical on either side of the middle of the pixel (Fig. 6a). This is not the case in the direction parallel to the x -axis (Fig. 6b), according to the guided mode spatial transients as discussed before. So, near the edge of the pixel corresponding to the beginning of the guided mode propagation, the temperature change is much lower than in the middle of the active region and nonlinear effects are strongly reduced.

The thermal resistance of a pixel, defined as the ratio of the mean temperature rise to the heating power is $R_{\text{th}} = 120 \text{ K W}^{-1}$. This value can be used to estimate the mean temperature variation for any value of the heating power density.

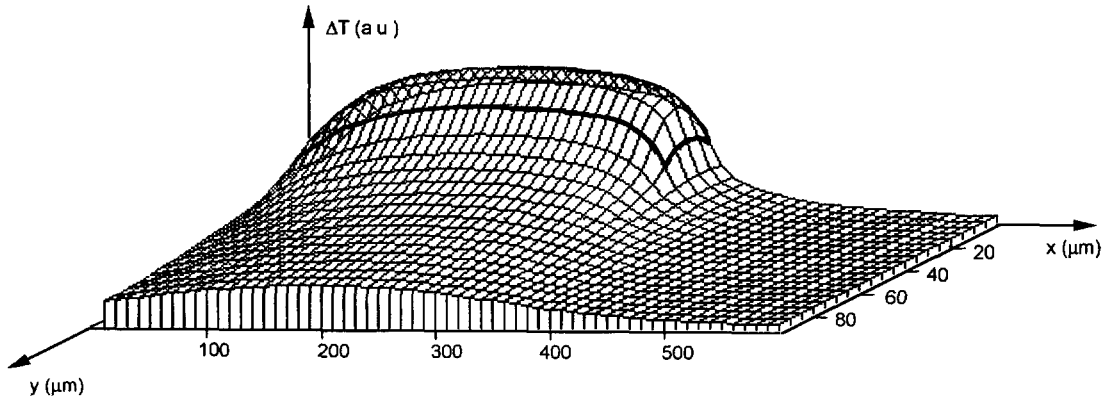


Fig. 5. — Temperature distribution around an active pixel

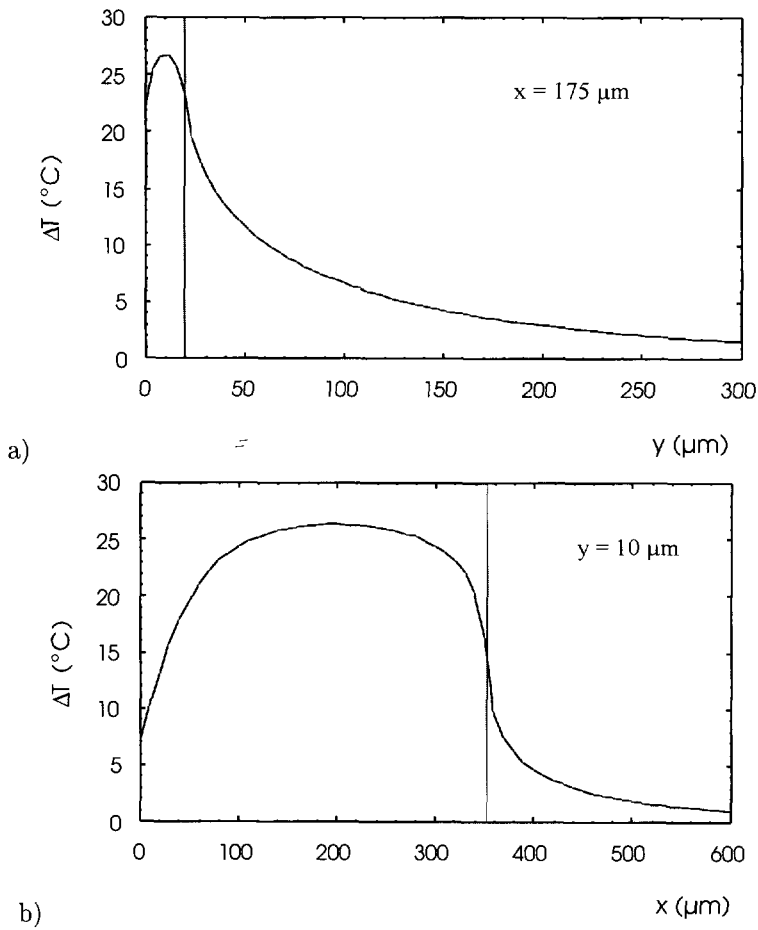


Fig. 6 — Temperature variations along the symmetry axes of the active pixel. a) in the transverse direction, parallel to the x -axis, b) in the longitudinal direction, parallel to the y -axis.

Outside the pixel, the temperature decreases and the calculation allows to estimate the minimum distance between two pixels to limit their thermal interaction. Considering the nearest neighbours, the mean temperature of a non-heated pixel is calculated as a function of its distance to the heated one. Along the x -direction, the mean temperature rise of a non heated pixel is $0.80\text{ }^{\circ}\text{C}$ for a distance of $500\text{ }\mu\text{m}$ between the pixel centers, which corresponds to 3.3% of the temperature variation of the heated pixel. Along the y -axis, a distance of $250\text{ }\mu\text{m}$ has been considered; the mean temperature rise is then $1.9\text{ }^{\circ}\text{C}$, which is 7.8% of the mean temperature rise of the active pixel.

Assuming that one non-active pixel is surrounded by four heated pixel, excited at the switching threshold, and set at the distances previously mentioned, the maximum parasitic temperature rise induced on the central pixel can be estimated by adding the contribution of every heated pixels. This leads to $5.4\text{ }^{\circ}\text{C}$, which corresponds to 22.2% of the temperature increase needed for switching. This is low enough to prevent the central pixel from switching unexpectedly.

Such calculations of the temperature distribution induced by an active pixel have been used to design a logic gate array [8]

Conclusion

The image method, which is widely use to solve electrostatic problems, has been transposed to study heat diffusion in a logic gate array. The temperature distribution has been calculated over an active pixel surface and thermal interaction between neighbour pixels has been estimated. This has been used to determine the minimum distance between pixels to insure that thermal coupling do not affect the array operation.

Acknowledgments

The authors would like to thank P. Dansas for helpful discussions.

References

- [1] Bewtra N., Suda D.A., Tan G.L., Chatenoud F. and Xu J.M., Modeling of quantum-well lasers with electro-opto-thermal interaction, *IEEE J. of selected topics in Quantum Electronics* 1 (1995) 331.
- [2] Olbright G.R., Peyghambarian N., Gibbs H.M. Macleod H A. and Van Milgen F., Microsecond room-temperature optical bistability and crosstalk studies in ZnS and ZnSe interference filters with visible light and milliwatt powers, *Appl. Phys. Lett.* 45 (1984) 1031.
- [3] Thienpont H., Peiffer W., Nieuborg N., Veretennicoff I., de Tandt C., Ranson W., Vounckx R. and Koster A., Silicon Implanted Oxide multifunctional optical switches for smart pixel arrays, CLEO, Amsterdam, proc. (1994) p. 351.
- [4] Thienpont H., Peiffer W., Nieuborg N., Veretennicoff I., Ranson W., de Tandt C., Vounckx R., Koster A. and Laval S., Optical information processing planes with silicon technology, International Conference on Optical Information Processing, Saint-Petersbourg, 2-7 Août 1993 (Proceeding SPIE Vol. 2015, 1993) pp. 180-192

- [5] Downer M.C. and Shank C.V., Ultrafast Heating of Silicon on sapphire by Femtosecond Optical Pulses, *Phys. Rev. Lett.* **56** (1986) 761.
- [6] Lompré L.A., Liu J.M., Kurz H. and Bloembergen N., Optical heating of electron-hole plasma in silicon by picosecond pulses, *Appl. Phys. Lett.* **44** (1984) 3.
- [7] Feng S.T. and Irene E.A., Optical switching and optical logic in a thermally expanding Si etalon, *Appl. Phys. Lett.* **58** (1991) 2073
- [8] Gualous H., Koster A., Pascal D. and Laval S., Non optical logic gate array: fan-in and fan-out measurements, *International J. optoelectronics* **9** (1994) 471-476.
- [9] Janossy I., Gordon J., Mathew H., Abraham E., Taghizadeh M.R. and Smith D., Dynamics of thermally induced optical bistability, *IEEE J. Quantum Electronics* **QE-22** (1986) 2224.
- [10] Janossy I., Taghizadeh M.R., Gordon J., Mathew H. and Smith D., Thermally induced optical bistability in thin film devices, *IEEE J. Quantum Electronics* **QE-21** (1985) 1447-1452.
- [11] Leturcq P., Dorkel J.-M., Napieralski A. and Lachiver E., A new approach to thermal analysis of power devices, *IEEE Trans. Electron Devices* **34** (1987) 1147-1156.
- [12] Gualous H., Koster A., Pascal D. and Laval S., Guided wave spatial transients under a limited grating coupler in a silicon-on-sapphire waveguide, *Optics Commun.* **123** (1996) 83-88.
- [13] Gualous H., Étude et réalisation d'une matrice de portes logiques optiques à guide d'onde en silicium sur saphir, Thèse de Doctorat, n°3171 (Orsay, 1994)